REFLECT – Research Flight of EURADOS and CRREAT: Intercomparison of various radiation dosimeters onboard aircraft

Iva Ambrozova, Peter Beck, Eric Benton, Robert Billnert, Jean Francois Bottollier Depois, M. Caresana, Nesrine Dinar, Szymon Domanski, Michal Aleksander Gryzinski, Martin Kakona, et al.

REFLECT – Research Flight of EURADOS and CRREAT

Intercomparison of various radiation dosimeters onboard aircraft

Running head: Dosimeters' intercomparison onboard aircraft

Iva Ambrožová*[1], Peter Beck[2], Eric R. Benton[1,3], Robert Billnert[4], Jean-Francois Bottollier-Depois[5], Marco Caresana[6], Nesrine Dinar[7], Szymon Domański[8], Michał A. Gryziński[8], Martin Kákona[1,9], Antonín Kolros[10,11], Pavel Krist[1], Michał Kuć[8], Dagmar Kyselová[1,9], Marcin Latocha[2], Albrecht Leuschner[12], Jan Lillhök[4], Maciej Maciak[8], Vladimír Mareš[13], Łukasz Murawski[8], Fabio Pozzi[7], Guenther Reitz[1,14], Kai Schennetten[14], Marco Silari[7], Jakub Šlegl[1,9], Marek Sommer[1,9], Václav Štěpán[1], Francois Trompier[5], Christoph Tscherne[2], Yukio Uchihori[15], Arturo Vargas[16], Ladislav Viererbl[10,11], Marek Wielunski[13], Mie Wising[4], Gabriele Zorloni[6], Ondřej Ploc[1]

[1] Nuclear Physics Institute CAS, Czech Republic

[2] Seibersdorf Labor GmbH, Austria

[3] Oklahoma State University, USA

[4] Swedish Radiation Safety Authority, Sweden

[5] Institute for Radiological Protection and Nuclear Safety, France

[6] Politecnico di Milano, Italy

[7] CERN, Switzerland

[8] National Centre for Nuclear Research, Poland

[9] Faculty of Nuclear Sciences and Physical Engineering CTU, Prague, Czech Republic

[10] Research Centre Rez, Czech Republic

[11] HHtec Association, Czech Republic

[12] Deutsches Elektronen-Synchrotron, Germany

[13] Helmholtz Zentrum München, Germany

[14] German Aerospace Center, Germany

[15] National Institute of Radiological Sciences / QST, Japan

[16] Technical University of Catalonia, Spain

* ambrozova@ujf.cas.cz, Nuclear Physics Institute CAS, Department of Radiation Dosimetry, Na Truhlarce 39/64, Prague, 18000, Czech Republic

Abstract

Aircraft crew are one of the groups of radiation workers which receive the highest annual exposure to ionizing radiation. Validation of computer codes used routinely for calculation of the exposure due to cosmic radiation and the observation of nonpredictable changes in the level of the exposure due to solar energetic particles, requires continuous measurements onboard aircraft. Appropriate calibration of suitable instruments is crucial, however, for the very complex atmospheric radiation field there is no single reference field covering all particles and energies involved. Further intercomparisons of measurements of different instruments under real flight conditions are therefore indispensable.

In November 2017, the REFLECT (**RE**search **FL**ight of **E**URADOS and **C**RREA**T**) was carried out. With a payload comprising more than 20 different instruments, REFLECT represents the largest campaign of this type ever performed. The instruments flown included those already proven for routine dosimetry onboard aircraft such as the Liulin Si-diode spectrometer and tissue equivalent proportional counters, as well as newly developed detectors and instruments with the potential to be used for onboard aircraft measurements in the future. This flight enabled acquisition of dosimetric data under well-defined conditions onboard aircraft and comparison of new instruments with those routinely used.

As expected, dosimeters routinely used for aircraft dosimetry (such as a tissue equivalent proportional counter (TEPC) or a silicon detector device like Liulin agreed reasonable with each other as well as with model calculations. Conventional neutron rem counters underestimated neutron ambient dose equivalent, while

extended-range neutron rem counters provided results comparable to routinely used instruments. Although the response of some instruments, not primarily intended for the use in a very complex mixed radiation field such as onboard aircraft, was as somehow expected to be different, the prove of their suitability was one of the objectives of the REFLECT. This campaign comprised a single short flight. For further testing of instruments, additional flights as well as comparison at appropriate reference fields are envisaged. The REFLECT provided valuable experience and feedback for future experiments.

Keywords

cosmic radiation; aircraft; dosimeter; intercomparison; research flight

1. Introduction

Aircraft crew and airline passengers are exposed to elevated dose rates due to cosmic radiation onboard aircraft; aircraft crew is considered as a group of workers receiving one of the highest annual effective doses (ICRP, 1991; ICRP, 2007; ICRP, 2016; IAEA 2003). Radiation protection for aircraft crew has been regulated in the European Union since 1996 by the EU-Directive 29/96/EURATOM (EURATOM 1996). Since then, this directive was updated with the EU-Directive 2013/59/EURATOM (EURATOM 2013). The EU member states were obliged to comply with the new regulations by updating their national legislations by February 2018. Annual personal doses from galactic cosmic radiation (GCR) to aircraft crew members are routinely calculated by various computer codes that are validated preferably by measurements but also by code intercomparisons. Ongoing validations of such codes need in-flight measurements with appropriately calibrated instruments.

An assessment of aircraft crew radiation exposure is a complex task. Radiation field at civil flight altitudes is formed by interactions of mainly GCR (and sporadically solar energetic particles – SEP) with the atoms of the atmosphere of the Earth. All types of particles and electromagnetic component such as protons, muons, pions, electrons, neutrons, gamma rays and others of a wide range of energies covering several orders of magnitude are present as primary or secondary radiation (Schraube 2000; ISO 2001; Lindborg et al. 2004). Depending on altitude and geomagnetic latitude, about 40 % - 70 % of ambient dose equivalent $H^*(10)$ is due

94 to neutrons, 20 % - 30 % due to electrons, 10 % due to protons and 10 % due to
95 photons and muons (Schraube et al. 2002a; Lindborg et al. 2004). In addition,
96 radiation field in the atmosphere is not constant in time and space due to solar
97 modulation of the GCR, strong variations of particle fluences and energies in
98 occasional SEPs, latitude effects caused by the geomagnetic field and build-
99 up/absorption effects resulting from nuclear reactions with the atmospheric nuclei.

100 An assessment of the radiation exposure of aircraft crew requires a determination
101 of the radiation protection quantity effective dose *E* (ICRP 2007). Since the effective
102 dose is not a measurable quantity, for operational radiation protection purposes, an
103 operational quantity, the ambient dose equivalent $H^*(10)$ was introduced (ICRU
104 1993). $H^*(10)$ should be a conservative estimate of *E*. An empirical determination of
105 $H^*(10)$ onboard aircraft requires accurate measurements using radiation detectors
106 sensitive to the different particles and energy ranges. The most important species
107 are neutrons (from few hundred keV up to few GeV) as they deliver the largest
108 fraction of dose. The $H^*(10)$ can be measured with an instrument suitably calibrated
109 for this quantity what is not a trivial task for instruments to be used in atmospheric
110 radiation field. For the very complex atmospheric radiation field, with its broad
111 range of different particles and energies, there exists no single reference field
112 covering all those radiation components. ISO reference radiation fields do not fully
113 cover the whole particle and energy range of interest (ISO 2012). Additionally, for
114 proper calibration, instrument responses for all particles and energies shall be taken
115 into account. To simulate a cosmic radiation field or some of its components at
116 aviation altitude, an accelerator-produced field such as provided at CERN EU High

Energy Reference Field (CERF) facility (Silari and Pozzi 2017; Pozzi et al. 2017, Pozzi and Silari 2019) or fields at high-mountains could be also used. However, the composition and spectra of these fields are not exactly the same as the one present onboard aircraft. Today, well calibrated Tissue Equivalent Proportional Counters (TEPC) are considered as the instruments that reasonably well approximate the operational dose quantity ambient dose equivalent in atmospheric radiation field (ISO 2012, Lindborg 1999). Other instruments need to be calibrated in appropriate reference fields or in situ against a TEPC.

Many in-flight measurements with different instruments were performed in the past and an overview of the most important research projects in aviation dosimetry during 1997-2007 was given in (Beck 2009). Further descriptions and results from various measurement campaigns onboard aircraft between 1992 and 2003 have been summarized in (Lindborg et al. 2004). Such measurements were usually done on single flights with changing altitude and cut-off rigidity (Bottollier-Depois et al. 2004; Kubančák et al. 2015). For constant flight conditions, measurements have been conducted with only a limited number of instruments, such as TEPC and silicon spectrometers (Meier et al. 2016; Lindborg et al. 2007; Latocha et al. 2007; Lillhök et al. 2007). Recently several new detectors that are potentially suitable for onboard aircraft dosimetry have been developed, but not yet fully tested in the field (Bottollier-Depois et al. 2019; Yasuda et al. 2020; Kakona et al. 2019).

Despite the measurements performed so far, there is still need for continuous measurements onboard aircraft especially for observing short-term variations of radiation levels associated with SEP. The silicon spectrometer Liulin has been used

onboard aircraft for many years. Several Liulin detectors are permanently installed onboard aircraft of Air France and Czech airlines (Ploc et al. 2013) although their sensitivity to neutrons is rather low and they are not tissue-equivalent. A TEPC (e.g. like Hawk-type) is typically not used for long-term measurements due to its rather large dimensions and relatively high power consumption. A unique exception is long-term TEPC measurements reported by (Beck et al, 2005) where the "Halloween Storms" between October and November 2003 were recorded.

Intercomparisons with different types of instruments, which are usually calibrated in different ways, are necessary. A comparison exercise employing different instruments conducted in regular time intervals (e.g. every few years) represents an independent form of a quality control for participating groups. In addition, in a view of a growing demand for increasing the quality of dosimetric measurements at aviation altitudes by the space weather community (Tobiska et al. 2015; Meier et al. 2018) measurement campaigns onboard aircraft are necessary.

In November 2017, the research campaign REFLECT (**RE**search **FL**ight of **E**URADOS and **C**RREA**T**) was carried out by Nuclear Physics Institute CAS. The response of more than 20 different detectors was investigated during a flight onboard a small aircraft. The instruments' ensemble included those already proved for dosimetry onboard aircraft such as Liulin and TEPCs, as well as newly developed detectors and instruments with the potential to be used for onboard aircraft measurements in future. Dosimetric data under well-defined conditions, including constant altitude and constant space weather conditions, were acquired. Sixteen institutes participated, several of them representing the leading research groups in aviation

dosimetry in their respective countries. As a result, REFLECT is the largest campaign of this type ever performed. This campaign was part of the research activities of Working Group 11 of EURADOS (EURADOS 2020) and of the CRREAT (Research Center of Cosmic Rays and Radiation Events in the Atmosphere) project (CRREAT n.d.).

2.Instruments

Radiation detectors included in the REFLECT campaign embraced instruments routinely used for cosmic radiation monitoring (TEPC, Liulin), newly developed radiation detectors as well as detectors with future potential for cosmic radiation monitoring onboard aircraft. With one exception, all instruments were active radiation detectors, i.e. electronic instruments capable of making time-resolved measurements.

An overview of the detectors used listing instruments, measured quantities, typically used radiation fields and participating institutes is given in Table 1. The detectors routinely used are underlined. Others are various neutron rem-counters, Si-detectors, recombination chamber or scintillation detectors.

Table 1. Instruments used during REFLECT

Instrument	**Quantity measured/ provided**	**Typical radiation field**	**Institute**

TEPC Hawk	$H^*(10)$	Mixed radiation	Institute for Radiological Protection and Nuclear Safety, France (IRSN) Seibersdorf Laboratories, Austria (SL)
Sievert instrument	$H^*(10)$	Mixed radiation	Swedish Radiation Safety Authority, Sweden (SSM)
Liulin	$D(Si)$, $H^*(10)$	Mixed radiation	Nuclear Physics Institute of the CAS, Czech Republic (NPI) National Institute of Radiological Sciences, QST, Japan (QST) German Aerospace Center, Germany (DLR)
REM-2 recombination chamber	$H^*(10)$	Mixed radiation	National Centre for Nuclear Research, Poland (NCBJ)
LB 6419	$H^*(10)$	Mixed radiation Neutrons (thermal – 300 MeV), photons	Deutsches Elektronen-Synchrotron, Germany (DESY)
TTM low-level neutron and gamma	$H^*(10)$	Mixed radiation	National Centre for Nuclear Research, Poland (NCBJ)

monitoring station			
Airdos	*D(Si)*	Mixed radiation	Nuclear Physics Institute of the CAS, Czech Republic (NPI)
Minipix	*D(Si)*	Mixed radiation	Nuclear Physics Institute of the CAS, Czech Republic (NPI)
NM2B-495Pb	$H^*(10)$	Neutrons (up to 10 GeV)	Helmholtz Zentrum München, Germany (HMGU)
LINUS	$H^*(10)$	Neutrons (up to 2 GeV)	European Council for Nuclear Research, Switzerland (CERN)
LB6411	$H^*(10)$	Neutrons (up to 20 MeV)	Nuclear Physics Institute of the CAS, Czech Republic (NPI)
Passive REM counter	$H^*(10)$	Neutrons	Politecnico di Milano, Italy (Polimi)
ELDO	$H_p(10)$	Neutrons (up to 200 MeV)	Helmholtz Zentrum München, Germany (HMGU)
HammerHead HH	$H^*(10)$	Photons (50 keV – 8 MeV), electrons, protons, muons, pions	HHtec for HHtec Association, Czech Republic (HHtec)

FH 40 G-10 with FHZ-612B probe	$H^*(10)$	Photons	National Centre for Nuclear Research, Poland (NCBJ)

2.1 Tissue equivalent proportional counters (TEPC)

A TEPC has the ability to provide values of the dose equivalent in tissue-equivalent material from most radiation components reasonably well. It is therefore particularly useful in comparisons of cosmic radiation measurements onboard aircraft (EURADOS 1996). Several different TEPCs were used to measure the dose equivalent during the REFLECT.

2.1.1 Hawk environmental Monitoring System FW-AD

The Hawk environmental Monitoring System FW-AD is a tissue equivalent proportional counter from Far West Technology Inc. (Goleta, California, USA), composed of a spherical chamber (127 mm diameter) with a wall from A-150 tissue equivalent plastic (2 mm thick) and filled with pure propane gas at low pressure (about 9.33 hPa) simulating of 2 µm site size (Conroy 2004). The outer container is made of 6.35 mm thick stainless steel. The dose equivalent is calculated from a spectrum of single energy deposition events and a radiation quality factor Q, determined by the $Q(L)$ relation given in (ICRP 60), where L denotes the unrestricted linear energy transfer (LET) in the exposed material (ICRP 2007).

Both IRSN and SL used Hawk type 1 systems using two linear multichannel analyzers working in parallel with low and high gains. The low-gain analogue to digital converter (ADC) measures LET spectra up to 1024 keV·µm^{-1} with 1 keV·µm^{-1} resolution. The high-gain channel uses an ADC measuring up to a lineal energy of 25.6 keV·µm^{-1} with a resolution of 0.1 keV·µm^{-1}. The energy deposition of the low and high LET components and the associated quality factor are stored in an output file once per minute. The separation between the low and the high LET component is set at 10 keV·µm^{-1} according to the *Q(L)* relationship (ICRP 2007). Events, encountering significant electronic noise, below the so-called low energy threshold (0.3 keV·µm^{-1} for IRSN and 0.5 keV·µm^{-1} for SL) are not recorded. An extrapolation function based on ^{60}Co gamma-rays LET spectrum was chosen for the SL Hawk. For the IRSN Hawk data analysis, a simple coefficient (the average of correction factor determined for ^{60}Co and ^{137}Cs gamma-rays) was applied (Farah et al. 2017). No compensation of the counting loss due to dead time is included in the analysis software.

Correction factors, N_{low} and N_{high} to ambient dose-equivalent for the low and high LET components of the dose equivalent are used. N_{low} was determined in photon radiation fields with ^{60}Co and ^{137}Cs sources. N_{high} was defined using the neutron reference sources of ^{241}Am-Be or ^{252}Cf neutron sources. The values of N_{low} are 1.11±0.02 and 1.34 ± 0.03 and the values of N_{high} are 0.80±0.09 and 0.84 ± 0.10 for IRSN and SL, respectively. Correction coefficients for neutrons were also evaluated for between 0.5 and 19 MeV and were found similar to Am-Be or ^{252}Cf neutron sources (Trompier et al. 2007).

2.1.2 Sievert instrument

The Sievert instruments are microdosimetric detectors developed by SSM (Kyllönen et al. 2001a; Lillhök et al. 2017). The detectors are TEPCs with 5 mm A-150 walls housed in vacuum containers of 2 mm aluminum. The detector volume has a diameter and length equal to 11.54 cm and a volume of 1207 cm^3. The detectors are working at a gas pressure of 1.3 kPa of propane based tissue-equivalent gas with (volume fractions) 55% C_3H_8, 39.6% CO_2 and 5.4% N_2, to simulate an object size with a mean chord length of 2 µm.

The electric charge is integrated for an integration time of typically 0.1 to 0.3 s. The absorbed dose to detector gas during this time interval is calculated from the average charge, the mass of the detector gas, the mean energy required to create an ion pair (an average value of 27.2 eV was used in the analysis), and the detector gas multiplication factor.

Characterization of the radiation quality is based on the variance-covariance method (Kellerer 1968; Bengtsson 1970; Lindborg and Bengtsson 1971; Kellerer and Rossi 1984).

In cosmic radiation applications where the high-LET events are rare and the absorbed dose rate is relatively low, a mixed single-event and multiple-event analysis can be used (Kyllönen et al. 2001b). The measured spectrum will in such situations have a region dominated by multiple events, and another region dominated by single high-LET events. The regions are chosen to be separated at 150 $keV \cdot \mu m^{-1}$. The quality factor in the multiple-event region (<150 $keV \cdot \mu m^{-1}$) is

calculated from the dose-average lineal energy by using a linear *Q(y)* relation. In the region above 150 keV·μm^{-1}, the events are treated as single events (after correction for a multiple-event contribution), y was set equal to L and the corresponding absorbed dose fraction multiplied by the quality factor defined in ICRP 103 (ICRP 2007). In addition, a correction factor $c_{Q,\,high} = 1.25$ for the high-LET component below 150 keV·μm^{-1} for the difference between the *Q(y)*-function used and $Q(L)$ according to ICRP60 is obtained from a previous comparison of the two approaches on aircraft measurements (Lillhök et al 2007).

From Monte Carlo (MC) simulations of the neutron detector response (Lillhök 2007) using a simulated atmospheric neutron spectrum (Roesler et al 1998) the detector absorbed dose and the ambient absorbed dose $D^*(10)$ agree within 3%.

The low-LET and high-LET components are defined as the contribution with dose-average lineal energy 1.6 keV·μm^{-1} measured with these detectors in a ^{60}Co gamma radiation field, and 94 keV·μm^{-1} simulated for these detectors in a simulated atmospheric neutron spectrum (Lillhök 2007).

2.2 Other detectors for mixed radiation fields

2.2.1 Liulin

The Mobile Dosimetry Unit (MDU) Liulin is a silicon semiconductor spectrometer that has been used for cosmic radiation measurements (Dachev 2009) as well as aircraft crew dosimetry for many years (Ploc et al. 2013; Meier et al. 2009). Liulin is equipped with a Hamamatsu S2744-08 PIN diode (10 x 20 x 0.3 mm^3), low noise

hybrid charge-sensitive preamplifier AMPTEK Inc. type A225, fast 12-bit analogue-digital converter (ADC), 2 or 3 microcontrollers and flash memory. Liulin detects energy imparted to its active volume in a single energy deposition event. Pulse amplitudes are stored in a 256-channel spectrum (only 8 most significant bits are used from ADC), from which the absorbed dose in silicon is then calculated. The energy calibration of Liulin was obtained at HIMAC (Uchihori et al. 2002).

Liulin can also be used to estimate $H^*(10)$ onboard aircraft, using the absorbed dose in silicon and an appropriate conversion factor, which can be determined by various means (Ploc et al. 2011; Wissmann and Klages 2018). In this experiment, several MDU models were used; however, $H^*(10)$ is given only for Liulin MDU7 (NPI). MDU7 was recently calibrated at CERF, which enabled to obtain calibration coefficient converting D_{Si} to $H^*(10)$ as described for example in Ploc et al. (2011).

2.2.2 Airdos

Airdos is detector with similar design and sensitivity as Liulin. It has been designed as open source instrument for measurement in mixed radiation fields with low intensity such as those encountered onboard aircraft (Kakona et al., 2019). It is composed of a silicon PIN diode (Hamamatsu S2744-09) of the same type used in the Liulin MDU, electronics for converting the signal to the pulse-height spectra, a GPS module, an SD memory card and batteries. Full documentation is freely available at (GitHub, 2020). In this measurement campaign, a version Airdos 01 was used. Energy range of Airdos 01 is from 0.2 to 12.5 MeV of deposited energy in silicon with energy resolution 49.4 keV per channel. Accumulated pulse amplitudes

284 are stored in 250 channels spectra every 15 seconds. The detector was calibrated
285 using heavy charged particle beams at HIMAC (NIRS, Japan) and at the U-120M
286 cyclotron (NPI, Czech Republic).

287 2.2.3 Timepix

288 Timepix (Llopart et al. 2002; Llopart et al. 2007) is a hybrid semiconductor pixel
289 detector which consists of matrix of 256 x 256 pixels (total of 65536 pixels).
290 Timepix was developed by Medipix2 collaboration (Campbell 2011). The pixel pitch
291 is 55 μm and total sensitive area is nearly 2 cm^2. For this flight the silicon with
292 thickness of 500 μm was used as a semiconductor sensor chip. The Timepix chip
293 was readout by compact electronics which is in MiniPIX interface (Granja 2018,
294 Granja and Pospisil 2014). The detector was operated in per-pixel energy mode
295 which allows to measure the time that the signal spent over threshold. The
296 calibration between time over threshold to deposited energy was done by method
297 described in (Jakubek 2011). Due to high granularity provided by Timepix
298 architecture the detector can measure single particle energy deposition events
299 (Granja and Pospisil 2014). The configuration of Timepix device and data
300 acquisition (including the pre-processing of data) was performed in PIXET software
301 (Turecek 2015) which was run on standard Windows laptop.

302 2.2.4 REM-2 recombination chamber

303 The REM-2 is a cylindrical parallel-plate recombination chamber with an active
304 volume of about 1800 cm^3 and total mass of 6.5 kg. The chamber has 25 tissue-

equivalent electrodes and it is filled with the gas mixture consisting of methane and 5% nitrogen, with high pressure up to 1 MPa. The effective wall thickness (Al) of the chamber is equivalent to about 1.8 cm of tissue. The REM-2 chamber approximates the dosimetric parameters of the ICRU sphere in such a way, that the dose contribution and energy spectrum of secondary charged particles in the chamber active cavity are similar to those in the ICRU sphere at the depth of 10 mm (Maciak 2018). Therefore it can be used for the determination of $H^*(10)$ in mixed radiation fields (Zielczyński et al. 2008; Caresana et al. 2014; Murawski et al. 2018).

The chamber is designed in such a way that the initial recombination of ions occurs when the chamber operates at polarizing voltages below saturation and, for a certain range of gas pressure and dose rates, the initial recombination exceeds volume recombination. Measuring methods are based on the determination of the dose rate from the saturation current and the radiation quality from the amount of initial recombination. By means of recombination methods it is possible to estimate the radiation quality factor (Zielczyński et al. 1994; Golnik et al. 2004; Golnik 2018).

The method used for the determination of the radiation quality involves measurements of two ionization currents i_S and i_R at two properly chosen polarizing voltages U_S and U_R. A certain combination of these two currents is called recombination index of radiation quality Q_4 and may serve as a measurable quantity that depends on LET in a similar way as the radiation quality factor does (Golnik 2018). The polarizing voltage U_S is the high voltage, the same as for the measurements of the absorbed dose. The lower voltage U_R, called the recombination voltage~~,~~ has been determined during calibration of the chamber in a reference

gamma radiation field of air kerma from ^{137}Cs source. U_R ensures 96% of ion collection efficiency in such reference field. The ambient dose equivalent is calculated as the product of absorbed dose and Q_4.

The detector was calibrated at CERF in 2016, and twice in monoenergetic neutron reference fields: at PTB (Golnik et al. 1997) and in 2018 at NPL. Before the REFLECT measurements, the chamber was calibrated at 990 V saturation voltage in the accredited (AP 070) Radiation Protection Measurements Laboratory (LPD, NCBJ) according to the Operational procedure M-1 (2017) with a ^{137}Cs reference photon source and PuBe reference neutron source.

2.2.5 TTM low-level neutron and gamma monitoring station

The low-level neutron and gamma monitoring station registers photons and neutrons in separate 'pulse-height' windows (Pszona et al. 2014). The detector is based on an 8 inch Leake neutron area survey instrument (Leake et al. 2004). It uses a Centronic SP9 ^{3}He spherical proportional counter, surrounded by an inner polyethylene layer, a spherical shell of natural cadmium and a further outer polyethylene moderator. The cadmium shield is composed of two hemispherical shells, 0.91 mm thick, with 25 holes. The areas covered by the holes are the same in both hemispheres, except for a 12.5 mm hole used by the SP9 connector (Tagziria et al. 2004). Discrimination between photons and neutrons is based on the analysis of the pulse-height spectrum, defining the photon and neutron windows (Pszona et al. 2014). The neutron response function is shown in Figure 1. The TTM station was calibrated with ^{137}Cs and AmBe reference sources in the accredited (AP 070)

Radiation Protection Measurements Laboratory (LPD, NCBJ). Calibration factors used for the measurement were 0.55 nSv and 1.28 nSv per count for the photon and neutron windows, respectively.

2.2.6 LB 6419

The LB 6419 was designed by DESY and Berthold Technologies to measure the ambient dose equivalent $H^*(10)$ of pulsed and continuous neutron and photon radiation at high-energy accelerators (Leuschner et al. 2017). The LB 6419 comprises a cylindrical moderated rem-counter with a ^{3}He proportional counter and a plastic scintillator.

The response to low-energy neutrons H_{LEN} is obtained from the proportional counter by counting the reaction products of the nuclear reaction ^{3}He(n,p)T. Its moderator is made of polyethylene and contains neither any response-shaping absorbers like Cd or B nor converters like Pb. So it measures H_{LEN} with a calibration factor of 0.1 nSv per count. Its neutron response function is shown in Figure 1.

The response to high-energy neutrons H_{HEN} is obtained from the scintillator by collecting scintillator light above 20 MeV, a threshold where any response from electro-magnetic radiation such as γ, $e^{\pm}$, $\mu^{\pm}$ can be discriminated. The response comes from the energy deposition of charged products from neutron scattering on hydrogen nuclei of the scintillator H(n,n)p and on carbon nuclei as C(n,p) and C(n,α). As this response is based on the measurement of absorbed energy rather than counting it cannot be shown in Figure 1. The corresponding calibration factor was measured and validated at CERF in 2010, 2012 and 2017.

The total neutron dose H_N is obtained by summing up the doses of the two energy ranges H_{LEN} and H_{HEN}.

Electromagnetic radiation (H_{ELM}) can be separated from the neutron response because it shows up in the energy spectrum as the so called “muon peak”. In the cylindrical scintillator with its dimension of 4.1 cm these minimum ionizing particles lose about 8 MeV (2 MeV·cm^{-2}). The calibration is done by means of the Compton edges of radioactive sources such as ^{137}Cs and ^{60}Co.

Finally the total dose H_{TOT} is obtained by summing up the neutron dose H_N and the dose of the electro-magnetic radiation H_{ELM}.

2.2.7. HammerHead HH

The HammerHead HH (HHtec Association, Czech Republic) is a wide-range scintillation detector designed for high-precision $H^*(10)$ measurements. The ambient dose equivalent rate range is from 5 nSv·h^{-1} to 10 mSv·h^{-1} for a photon energy range from 50 keV to 8 MeV. The typical type A uncertainty is 12 % for 1 s measuring interval (1σ and $H^*(10)_{\text{terrestrial}}$ = 130 nSv·h^{-1}). The HH meter is a portable detector with dimensions of ø 80 mm x 340 mm and mass of 1.6 kg.

The HammerHead HH has been designed in order that the measured value best corresponds to the physical definition of $H^*(10)$ for photons and meet the strict criteria required by IEC 60846 for ambient dose equivalent meters. As detector, a CaF_2:Eu scintillator with low atomic number is used. It shape is close to a sphere of 64 mm diameter, therefore the meter has excellent -135° to +135° angular response. The HH meter works in current mode, therefore the measurement is not

394 influenced by dead time. The unique time-energy analysis of the measured signals
395 makes it possible to distinguish the contribution $H^*(10)_L$ from particles with energy
396 below 4 MeV and $H^*(10)_H$ from particles with energy above 4 MeV. When measuring
397 on the Earth's surface, the $H^*(10)_L$ value represents the terrestrial component of the
398 radiation field, whereas the $H^*(10)_H$ value allows estimating the secondary cosmic
399 ray component but without the influence of neutrons. The typical duration of a
400 measurement is 9 hours when the instrument is connected to a tablet for data
401 transfer.

402 HammerHead HH was calibrated in the accredited calibration laboratory at Czech
403 Metrology Institute in Prague with a X-ray device (40 keV - 250 keV) and ^{137}Cs, ^{60}Co
404 reference sources in terms of $H^*(10)$.

405 2.2.8 FH 40 G-10 with FHZ-612B probe

406 The FH 40 G-10 is a portable dose rate meter based on an internal energy filtered
407 proportional counter. Without any external probe connected, this device is sensitive
408 to photons only. During this experiment, an additional FHZ-612B Beta Gamma
409 probe was connected. Even with the external FHZ-61B connected, the detector was
410 used as gamma detector since the beta detector cap was installed. The $H^*(10)$
411 measuring ranges of the FH 40 G-10 and FHZ-612B are 10 $nSv \cdot h^{-1}$ – 1 $Sv \cdot h^{-1}$ and 100
412 $nSv \cdot h^{-1}$ – 10 $Sv \cdot h^{-1}$, respectively. The energy range is 20 keV – 4.4 MeV for the FH 40
413 G-10 and 82 keV – 1.3 MeV for the FHZ-612B.

The instrument was calibrated in the accredited (AP 070) Radiation Protection Measurements Laboratory (LPD, NCBJ) with a ^{137}Cs reference source in terms of $H^*(10)$ (ISO 1999).

2.3 Neutron rem-counters and dosimeters

Several neutron dosimeters and rem-counters were used. The design of neutron rem counters is based mostly on the Andersson-Braun type (Andersson and Braun 1963) or Leake type (Leake 1966) and they measure the neutron ambient dose equivalent, $H^*(10)$.

Neutron fluence response functions of the used neutron detectors are shown in Figure 1. Response functions are usually calculated with MC codes; several energy points are validated through measurements in monoenergetic neutron fields.

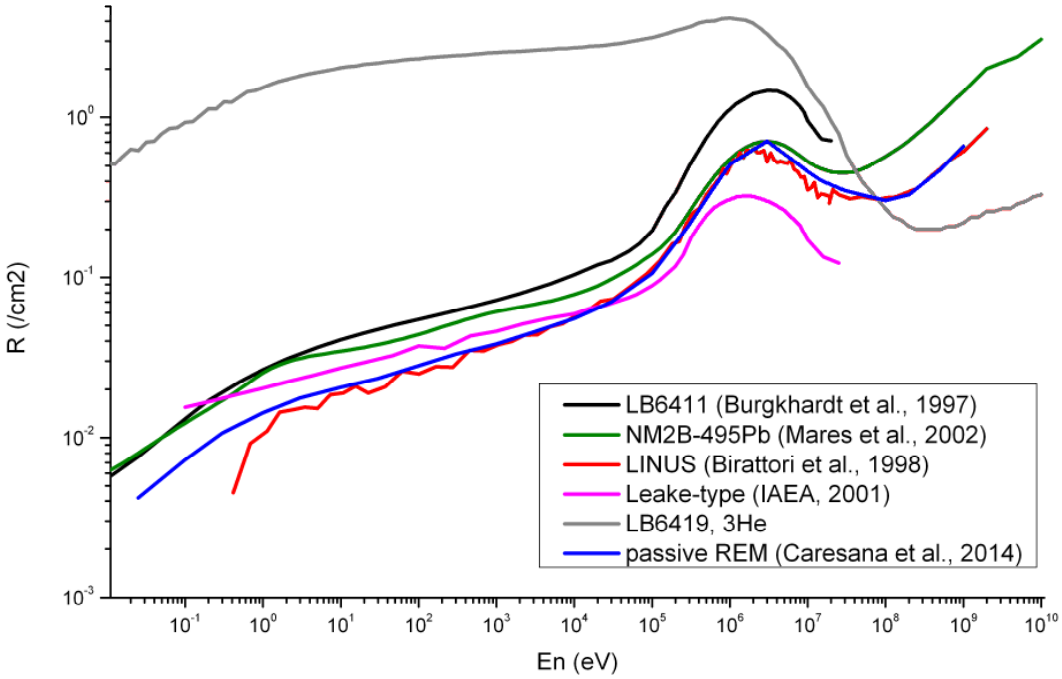

426

427 Figure1. Neutron response function R (counts per unit neutron fluence) of the neutron detectors

428 used in REFLECT.

429

430 ### 2.3.1 NM2B-495Pb Rem Counter

431 The NM2B-495Pb Rem Counter is based on the conventional Andersson-Braun rem-

432 counter (NE Technology Ltd.) with a cylindrical BF_3 proportional counter

433 surrounded by an inner polyethylene moderator, a boron-doped synthetic rubber

434 absorber, and an outer polyethylene moderator. To extend the detection range to

435 higher energy neutrons, a 1 cm thick lead shell is added around the boron rubber.

436 For this experimental flight, pulse height spectra were registered to control the

437 photon background and properly set up the region of interest (ROI). This procedure

438 enables an appropriate evaluation of the number of counts which are then

converted to $H^*(10)$ through the calibration coefficient. The fluence response function from thermal to 10 GeV neutrons was calculated by means of different Monte Carlo codes (Mares et al. 2002). The rem counter calibration was performed using a 185 GBq ^{241}Am-Be neutron source following the ISO recommendations (ISO 2001). The rem counter was also used and calibrated in 100 and 300 MeV quasi-mono-energetic neutron fields at RCNP in Osaka (Mares et al. 2017) and at CERF. The response function of the detector is shown in Figure 1.

2.3.2 LINUS

The LINUS (Birattari et al. 1990; Birattari et al. 1992; Birattari et al. 1993; Birattari et al. 1998) is the original extended-range rem counter. It consists of a ^{3}He proportional counter embedded in a spherical polyethylene moderator, which incorporates a boron-doped rubber absorber and a 1 cm thick lead shell so that its response function extends up to several hundred MeV. The signal is treated with a standard counting chain (pre-amplifier, amplifier, single channel analyzer and counter) and the TTL output is analyzed by a custom LabVIEW interface. The response function of the detector is shown in Figure 1. Neutron detectors are sensitive to some extend to gamma rays, which can transfer energy to the system through Compton scattering in the walls or fill gas. The gamma rejection for the LINUS is obtained by setting a discriminator below the low energy neutron signal to reject counts due to gamma rays and electronic noise. The threshold was determined by analyzing the pulse height spectrum of the ^{3}He counter.

460 The LINUS was calibrated with an AmBe source (Dinar et al. 2017) in the CERN
461 CALibration LABoratory (CALLAB) (Pozzi et al. 2015). The calibration provided a
462 calibration factor of 0.89 nSv per count with an overall uncertainty of 3.2% at one
463 sigma.

464 2.3.3 LB6411

465 The LB 6411 neutron probe (Burgkhardt et al. 1997), connected to the universal
466 monitor LB 123, is designed for measurement of neutron ambient dose equivalent
467 $H^*(10)$ in accordance with ICRP 60 (BERTHOLD n.d.). The LB 6411 consists of a
468 cylindrical ^{3}He proportional counter centered in a polyethylene sphere with
469 diameter 25 cm. The neutron energy range is from thermal to 20 MeV. The spectrum
470 from the bare ^{252}Cf neutron source has been used as the calibration spectrum. The
471 numerical calibration factor is 0.32 nSv per count (Burgkhardt et al. 1997). The
472 response function over the whole energy range was calculated with MCNP. For
473 several energies the results were crosschecked with monoenergetic neutron
474 measurements. The response function of the detector is shown in Figure 1. The
475 response to gamma radiation is approx. 10^{-3} counts per nSv, which means a
476 discrimination factor of 3×10^{3}.

477 2.3.4 Passive REM counter

478 The neutron contribution to $H^*(10)$ was also measured with a system consisting of
479 two CR-39 detectors 3x4 cm^2 in dimension coupled to a ^{10}B enriched converter,
480 positioned inside a sphere made with polyethylene, lead, and cadmium. The ^{10}B is

481 contained in boron carbide (B_4C) deposited on an aluminum plate. The thickness of
482 the boron carbide is about 10 μm. The instrument is an extended range rem counter
483 and the response function is shown in Figure 1. The full description of the
484 instrument is in (Caresana et al. 2014) while previous experience in measuring
485 onboard aircraft is described in (Federico et al. 2015).
486 The plug, hosting the two CR39 detectors assembled with the boron converter, was
487 removed from the moderating sphere during the shipment, inserted into the sphere
488 immediately before take-off and removed immediately after landing.

489 A check of the calibration coefficient was performed at CERF in August 2017 and
490 resulted in 10.6 $cm^{-2} \cdot \mu Sv^{-1}$ with an uncertainty equal to 14% (k=1). The sensitivity is
491 about 3 times higher than the one reported in (Caresana et al. 2014). This is because
492 the boron converter used in the above cited work is the Enriched Converter Screen
493 BE10 by Dosirad (France) whose thickness is about 100 μm. Using this converter,
494 only a layer of about 10 μm directly facing the CR39 detector contributes to the
495 signal, while interactions occurring at longer distance generate reaction products
496 that are self-absorbed in the converter. The effect is a depression of the thermal
497 neutron flux, resulting in a reduced sensitivity.

498 2.3.5 Electronic neutron dosimeter ELDO

499 The ELDO is an individual dosimeter developed at the Helmholtz Zentrum München
500 (HMGU), sensitive to neutrons from thermal energies up to about 200 MeV
501 (Wielunski et al. 2004). It is a small (160 g, 115x60x16 mm^3) personal dosimeter
502 with a dose measurement range between 1 μSv and 10 Sv. Its operational lifetime is

503 about 400 hours. It consists of four Si PIN-diodes with LiF or polyethylene (PE)
504 converters encapsulated in lead or cadmium. The combination of diodes and
505 converter enables separate measurements of neutrons with one fast-sensor (PE)
506 operating in the 1–200 MeV neutron energy range, two delta-sensors (LiF)
507 functioning between 50 keV and 2 MeV, and one albedo-sensor (LiF) sensitive to
508 low-energy neutrons (<50 keV). Each sensor is sensitive to a certain neutron energy
509 range and has its own calibration factor. The measured dose and dose rate in terms
510 of the personal dose equivalent, $H_p(10)$ (an operational quantity for individual
511 monitoring for the assessment of effective dose), are also shown on its LCD display.
512 Calibration of the ELDO was done at PTB Braunschweig, Germany, in mono-
513 energetic neutron fields with energies between 138 keV and 14.8 MeV (Bergmeier
514 et al. 2013). Additionally, the ELDO was also tested in the reference field of CERN-
515 CERF providing high-energy fields similar to that of secondary cosmic rays at flight
516 altitudes (Wielunski et al., 2018) and at the Environmental Research Station "UFS
517 Schneefernerhaus" (2,650 m above sea level) close to the summit of the Zugspitze
518 Mountain, Germany (Volnhals, 2012). In these experiments, an excess in the
519 measured counts was observed which are due to protons. Although the fluence of
520 protons is only 6% of the neutron fluence, protons caused around 12% of the
521 measured counts. The sensor response to protons and muons could be calculated
522 with GEANT4 calculations (Volnhals 2012) which support the observation.

2.4 Calculations

Ambient dose equivalent rates for different particles can be calculated using various models; the overview of codes assessing radiation exposure of aircraft crew is given in (Bottollier-Depois et al. 2012). All these codes provide calculations for the GCR induced radiation field in aircraft flight altitudes agreeing within 20 % with reference measurements (Bottollier-Depois et al. 2012). In this publication, the EPCARD.Net code (Mares et al. 2009) was used for comparison.

2.4.1 EPCARD.Net

The European Program package for the Calculation of Aviation Route Doses (EPCARD) is a widely used program for estimating the exposure of aircraft crew. This code was developed at the Helmholtz Zentrum München (Schraube et al. 2002b) and further improved in a new object-oriented code EPCARD.Net (Mares et al. 2009). In 2010, EPCARD.Net ver. 5.4.3 Professional was approved for official use for assessing radiation exposure from secondary cosmic radiation at aviation altitudes by the German Aviation Authority (LBA) and the National Metrology Institute, Physikalisch-Technische Bundesanstalt (PTB).

EPCARD.net is based on the results of extensive FLUKA Monte Carlo (Ferrari et al. 2005; Böhlen et al. 2014) calculations of particle energy spectra of neutrons, protons, photons, electrons and positrons, muons, and pions at various depths in the atmosphere down to sea level for all possible values of solar activity and geomagnetic shielding conditions (Roesler et al. 2002). The primary particle spectra

544 used in the FLUKA calculations as well as the modulation potential describing solar
545 activity were based on the model of Badhwar and O'Neill (Badhwar 1997; Badhwar
546 et al. 2000).

547 To determine the dose rates at specific locations in the atmosphere during a flight,
548 the cut-off rigidity, the solar deceleration potential and the barometric altitude are
549 calculated to quantify geomagnetic shielding, solar activity and atmospheric
550 shielding. The EPCARD.Net parameter database includes energy-averaged dose
551 conversion coefficients, calculated by folding each single-particle fluence spectrum
552 with the appropriate dose conversion function (Mares et al. 2004; Mares and
553 Leuthold 2007), which depends on barometric altitude, cut-off rigidity, and solar
554 activity, since the shape of the particle energy spectra also depends on these
555 parameters. Ambient dose equivalent, $H^*(10)$, and effective dose, E, are calculated
556 separately for each particle, i.e. the dose contributions from neutrons, protons,
557 photons, electrons, muons, and pions are assessed individually.

558 More general information about EPCARD is available on the web site (EPCARD
559 2020), where a simplified on-line version of the EPCARD calculator for public use
560 can also be found.

3. Experiment

3.1 Flight

The radiation detectors were exposed aboard an Embraer Legacy 600 aircraft operated by ABS Jets. The aircraft, together with 250 kg of equipment and eight scientific staff, flew from Vaclav Havel Airport in Prague (50.1°N, 14.2° E) to the FL390 flight level, on the 29th November 2017. The flight took off at the airport at 13:06 UTC and reached stable flight conditions (barometric altitude 11871 ± 8 m, range from 11853 to 11893), latitude 50.41 ± 0.14 °N (range from 50.18 to 50.58), longitude 15.80 ± 0.27 ° E (range from 15.26 to 16.24) at 13:38 UTC. At this level, the aircraft circled over the northern part of the Czech Republic (the area is a reserved airspace that is commonly used for operating test flights) for 90 minutes and landed back at Prague Airport at 15:34 UTC. Navigation data (barometric altitude, latitude, and longitude) were taken from the aircraft record and GPS. The flight route and flight profile are shown in Figure 2 and Figure 3, respectively. The space weather conditions were stable during the whole flight and no short-term solar activity affected the results. Space weather situation can be assessed e.g. by neutron monitors (nmdb.eu). During the flight the variation in the count rates of the neutron monitor at Lomnicky Stit (the nearest neutron monitor) was below 0.5%, which indicates stable space weather conditions.

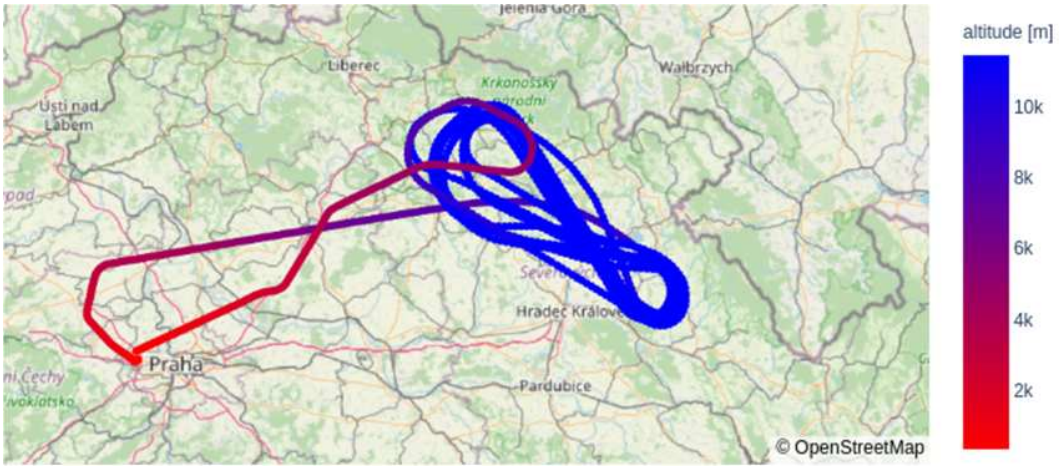

581

582 Figure 2. Flight route

583

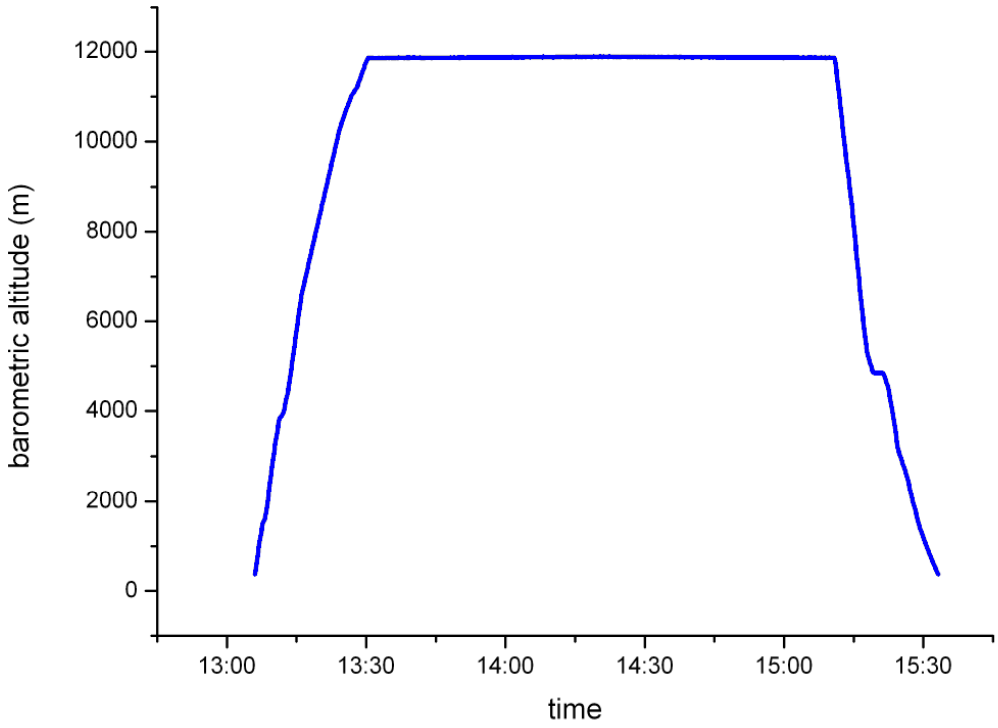

584

585 Figure 3. Flight profile

3.2 Location of detectors inside the aircraft

The detectors were placed at various locations inside the aircraft (Fig. 4). Equipment that needed power and manual control were installed on or behind the seats. Smaller devices like Liulins or Airdos were distributed in various locations inside the aircraft. The rest of the instruments were stored in the baggage compartment.

Two fuel tanks are located in the wings, two fuel tanks are in the bottom part of the body and two fuel tanks are in the rear part of the plane, behind the baggage compartment. Because the flight was quite short (about 2.5 hours), only the tanks in the wings were filled with fuel. The total amount of fuel before take-off was 5482 liters (4380 kg), 2530 kg were burned during the flight.

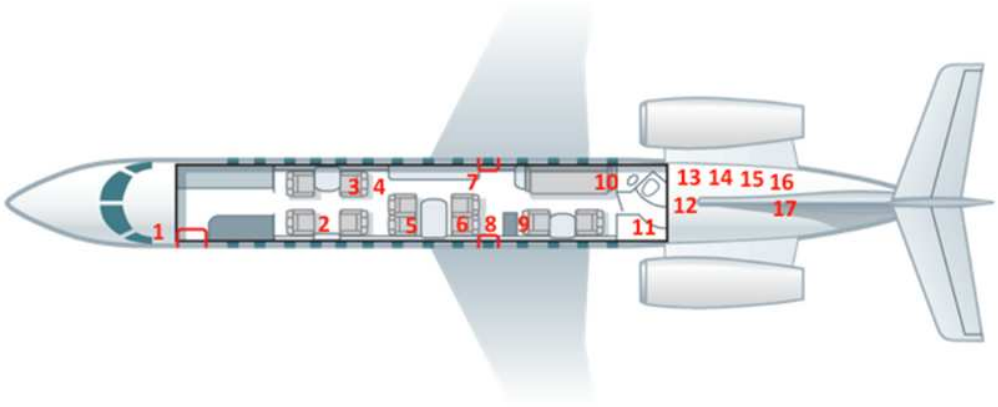

Figure 4. Placement of detectors inside the aircraft: 1 – Liulin MDU10; 2 – Sievert, 3 – Timepix; 4 – HammerHead; 5 – LB6411; 6 – LB6419; 7 – Liulin MDU7; 8 – NM2B-495Pb Rem Counter; 9 – Liulin

MDU14; 10 – LINUS; 11 – AIRDOS; 12 – REM-2 recombination chamber; 13 – TTM + FH 40 G-10 + FHZ-612B, 14 – ELDO; 15 – TEPC Hawk (IRSN); 16 – passive REM counter + Liulin MDU1; 17 – TEPC Hawk (SL).

4. Results and Discussion

Not all devices operated during the whole flight, part of the instruments were started when stable flight conditions were reached. To compare the results obtained with the active detectors, we consider only data acquired at a constant flight altitude.

Values of $\dot{H}^*(10)$ for various particles calculated with EPCARD are shown in Table 2. It should be noted that the calculations were done in free air, whereas the instruments measured inside the aircraft and therefore small differences can be expected due to shielding effects (Ferrari et al. 2004). As can be seen from Table 2, the most important contribution to $\dot{H}^*(10)$ is from neutrons (57% of the total $\dot{H}^*(10)$), followed by electrons (20%) and protons (15%). The uncertainty on the calculated values is estimated to be less than 20%, based on (Bottollier-Depois et al. 2012) who compared various codes used for assessing radiation exposure of aircraft crew due to GCR with the conclusion that the agreement between the codes was better than 20% from the median. The codes have also been previously validated by measurements with an agreement better than ±20 % (Lindborg, 2004).

Table 2. Calculated values of $H^*(10)$ rate during the REFLECT at FL390 for different particles using EPCARD.Net ver. 5.5.0

	neutrons	**photons**	**protons**	**electrons**	**muons**	**total**
$\dot{H}$***(10) [µSv/h]**	3.8 ± 0.8	0.3 ± 0.1	1.0 ± 0.2	1.3 ± 0.3	0.2 ± 0.0	6.6 ± 1.3

623

624 Table 3. Dose-equivalent rate measured with the various detectors. Uncertainties given as combined
625 uncertainties with k=1 and with the contribution from measurement statistics in parenthesis.

	Instrument	$\dot{H}$***(10) [µSv/h]**	$\dot{H}$***(10)$_{\text{Low-LET}}$** or $\dot{H}$***(10)$_{\gamma+e}$ [µSv/h]**	$\dot{H}$***(10)$_{\text{High-LET}}$** or $\dot{H}$***(10)$_{n}$ [µSv/h]**
routinely used instruments	TEPC HAWK (SL)	7.1 ± 0.5 (0.3)	3.3 ± 0.1 (<0.1)	3.8 ± 0.6 (0.3)
	TEPC HAWK (IRSN)	7.9 ± 0.6 (0.3)	3.5 ± 0.1 (<0.1)	4.4 ± 0.5 (0.3)
	Sievert (SSM)	7.4 ± 0. 6 (0.4)	2.9 ± 0.2 (0.1)	4. 5 ± 0.6 (0.6)
	Liulin MDU7 (NPI)	7.1 ± 1.1	3.1 ± 0.5	4.0 ±0.7
Neutron rem-counters	NM2B-495Pb (HMGU)			3.7 ± 0.4
	LINUS (CERN)			3.9 ± 0.1
	LB6411 (NPI)			2.1 ± 0.4
	Passive REM counter (Polimi)			7.5 ± 2.5

Others instruments	LB6419 (DESY)	9.1 ± 1.8	1.7 ± 0.4	7.4 ± 1.5
	REM-2 (NCBJ)	10.1 ± 8.9	–	–
	TTM (NCBJ)	4.8± 0.8	2.1 ± 0.4	2.8 ± 0.5
	ELDO (HMGU)			4.4 ± 0.9*
	HammerHead HH (HHtec Association)		2.7 ± 0.2	
	FH 40 G-10 (NCB)		3.2± 0.5	
	FHZ-612B (NCB)		4.7± 0.8	

626 * $H_P(10)$

627

628 Table 3 lists the measurement results (for all instruments except Si detectors
629 measuring only D_{Si}). The results are grouped in a low-LET component that
630 comprises the contribution of low ionizing radiation (photons, electrons, muons,
631 protons, pions) and in a high-LET component representing mostly contributions of
632 neutrons, stopping protons and higher Z ionizing particles. Even if the neutron
633 contribution can extend below 10 keV·μm^{-1} and for low energy photons it can be
634 above 10 keV·μm^{-1}, the previous assumption (high-LET assimilated to neutrons) is
635 usually made when comparing results of various instruments and calculations. One
636 should also note that most detectors designed for low-LET measurements exhibit a
637 response to neutrons that is usually unknown, especially for high-energy neutrons.

638 In the table, the results provided are not corrected for this unknown neutron
639 response. Uncertainties are given as combined uncertainties with contributions
640 from calibration and measurement statistics and presented with coverage factor
641 k=1. For TEPC, the statistical uncertainty is given in parenthesis. The first group
642 includes instruments routinely used onboard aircraft, measuring both low and high-
643 LET components, the second group includes neutron rem-counters and the third
644 group includes the remaining instruments.

645 When comparing the results, an agreement of ±20 % at a 95 % confidence level is
646 considered satisfactory. The recommendation on acceptable uncertainties in
647 radiation protection is given in (ICRP 1997) where it is stated: *"…overall uncertainty*
648 *at the 95 % confidence level in the estimation of effective dose around the relevant*
649 *dose limit may well be a factor of 1.5 in either direction for photons and may be*
650 *substantially greater for neutrons of uncertain energy and for electrons. Greater*
651 *uncertainties are also inevitable at low levels of effective dose for all qualities of*
652 *radiation.*"

653 The measurements of the various TEPCs (HAWK, Sievert) agreed well with each
654 other, with Liulin, and with the EPCARD calculations, as it was during a previous
655 flight comparison (CAATER) (Lillök et al 2007). The differences in low- and high-
656 LET components between the Sievert instrument and the other TEPCs were likely
657 due to the fact that the Sievert instrument distinguished $H^*(10)$ contributions from
658 photons and neutrons rather than in terms of a low and high-LET threshold. The
659 differences could have been also due to different locations of the TEPCs (Hawks in
660 the baggage compartment, Sievert in the front of the plane). During the

661 approximately 90 minutes of the cruise, the TEPC experienced statistically low
662 number of high LET events, which resulted in higher uncertainties for this
663 component.

664 The LB6419 and REM-2 measured larger values of total $H^*(10)$ than the TEPCs. The
665 REM-2 is very sensitive to vibrations, which probably led to the very high value of
666 the uncertainty. In principle, there are recombination methods for separating the
667 dose according to LET, but in this flight, the measurement method was simplified
668 because of the short time and difficult conditions. Provision of the values for the low
669 and high-LET components would be helpful to better interpret the data. Improved
670 calibration is needed to make use of REM-2 for routine aircraft dosimetry.

671 The LB6419 also measured a higher value of total $H^*(10)$ than the TEPCs. In
672 addition, Table 3 shows a small measured value of the low-LET radiation
673 contribution and an increased contribution of the high-LET component as compared
674 to the TEPCs. There is a need to check the separation method of the two components
675 and the calibration, since the total ambient dose equivalent was also too high
676 compared to the TEPC.

677 The $H^*(10)$ values measured with the TTM monitoring station, especially the
678 neutron component, was lower than the other instruments. Since only polyethylene
679 was used as a moderator (no lead or other high atomic number material was
680 included in the shell), the neutron energy range of this instrument was limited to
681 20 MeV.

682 Except for the LB6411 and TTM, the instruments measuring only the neutron
683 component provided results comparable to the TEPC results and with the EPCARD
684 calculations.

685 According to the EPCARD model, neutrons contributed for more than 50% to the
686 total $H^*(10)$; neutrons can reach energies up to several hundreds of MeV
687 (Pazianotto et al. 2017). Conventional neutron REM counters have a detection range
688 usually limited to about 15–20 MeV, their response dropping sharply at higher
689 energies. To extend the range to higher energies (up to several hundreds of MeV), a
690 shell of high-Z material (like tungsten or lead) is usually added to the PE moderator.

691 As expected, due to their response functions (Fig. 1), the LB6411 and TTM measured
692 lower values. This was in agreement also with measurements by Yasuda et al.
693 (2018), who investigated neutron doses during long-haul flights with two neutron
694 monitors and compared their results with JISCARD EX calculations. They found that
695 the relative contribution to $H^*(10)$ of neutrons with energies above 15 MeV could
696 exceed 50%.

697 The passive REM counter only provided an integral value over the whole flight (the
698 detector was installed inside the moderator just before take-off and removed after
699 landing). The total measured $H^*(10)$ was 15 ± 5 μSv; the dose rate at flight level
700 FL390 can be assessed assuming a taxi time of about 2 h and neglecting the small
701 contribution arising from the 0.5 h spent to reach the flight altitude and get back to
702 ground.

703 A possible explanation of the large measured $H^*(10)$ value is that the passive REM
704 counter – because of a misunderstanding with the shipping company – reached
705 Prague by airmail. Of course, the plug with the detector was not in the measuring
706 position, thus insensitive to fast neutrons. However, a small contribution from
707 thermal neutrons cannot be excluded.

708 Amongst the instruments measuring only the low-LET component, only the
709 HammerHead HH and the FH 40 G-10 obtained reasonable results. The results from
710 the other instruments disagreed with both the EPCARD calculation and the TEPC
711 measurements. It is difficult to compare the results because some photon detectors
712 are not only sensitive to photons and electrons, but also to protons, muons, pions
713 and to neutrons in some extend. For these instruments, their response to
714 components of the field other than that intended to be measured is not always
715 known.

716 Table 4 summarises the results of the silicon detectors (in terms of absorbed dose).
717 For these instruments, the dose in silicon was converted to dose in water using a
718 dose conversion factor of 1.23 (Ploc 2009). In a previous intercomparison flight
719 with Liulin MDUs (Meier et al. 2016) it was found that there could be differences in
720 the mass of the sensitive volume of the detectors (Si sensor size) considered in the
721 calculation of absorbed dose. In this experiment, we calculated the absorbed dose in
722 silicon using the same Si sensor mass (0.16597 g (Meier et al. 2016)) for all Liulin
723 units and for Airdos.

724 Table 4: Results (absorbed dose rate in silicon and in water) of the measurements with the Silicon
725 detectors

Instrument	MDU 7 Liulin (NPI)	MDU 10 Liulin (QST)	MDU14 Liulin (QST)	MDU1 Liulin (DLR)	Airdos T4 (NPI)	Minipix (NPI)
D_{Si} (μGy/h)	2.8 ± 0.2	2.1 ± 0.3	2.7 ± 0.5	2.0±0.3	1.8 ± 0.2	1.9 ± 0.3
D_{H2O} (μGy/h)*	3.4 ± 0.3	2.6 ± 0.4	3.3 ± 0.6	2.5±0.3	2.2 ± 0.2	2.3 ± 0.3

* The dose D_{H2O} was calculated from D_{Si} using a conversion factor 1.23

Although both Liulin and Airdos have similar sensitive volumes (mass, area, thickness), they have different properties such as energy range of deposited energy and width of the channel. Airdos has channel width of 49.4 keV whereas Liulin's is 81.4 keV. The energy range of Airdos (up to 12 MeV) is smaller than Liulin's (up to 24 MeV), in order to provide more detailed information on the lower part of the energy spectrum. The significant part of the deposited energy when measuring onboard aircraft comes from events depositing energy in the first several channels (for Liulins, 65–83% of the absorbed dose was due to events with deposited energy below 1 MeV, only 2–6% was due to events with deposited energy above 10 MeV).

To compare Airdos with Liulin, we considered only events within the energy range of Airdos for the calculation of absorbed dose for Liulin. For MDU 7, D_{Si} was 2.6 $\mu Gy \cdot h^{-1}$, for MDU 10 D_{Si} was 1.9 $\mu Gy \cdot h^{-1}$, and for MDU 14 D_{Si} was 2.6 $\mu Gy \cdot h^{-1}$, to be compared with 1.8 $\mu Gy \cdot h^{-1}$ measured by Airdos.

Some differences in the results could be due to the different shielding configurations (for example, the aircraft fuel acts as a good neutron moderator) around the locations in which the devices were installed (Fig. 4). The DLR Liulin was in the

743 baggage compartment, whereas the NPI Liulin and the Airdos were in the central
744 part of the aircraft or in the crew cabin. For Embraer Legacy 600, the baggage
745 compartment is located in the rear part of the aircraft, between the engines (Fig. 4).
746 Therefore, the baggage compartment, loaded with several larger instruments and
747 suitcases, is supposed to be more shielded than other areas of the aircraft. As was
748 shown in Ferrari et al. (2004), the shielding provided by the aircraft structure
749 (wings, engines, passengers, fuel) can cause a notable reduction in E or $H^*(10)$ for
750 most components of cosmic radiation. Differences in ambient dose equivalent for
751 various places inside the aircraft can be up to about 20% (Ferrari et al. 2004;
752 Battistoni et al. 2005; Kubancak et al. 2014). Nevertheless, the differences between
753 individual Liulin-type detectors seem to be too large to be explained only by
754 different locations in the aircraft. There appears to be some systematic differences.
755 The reason of these differences should be further investigated in comparison on
756 ground. Even for the detectors using the same Si diode, several factors can influence
757 the results, e.g. energy calibration, choice of the noise threshold, channel width
758 (Kakona et al. 2019).

759 Although the Minipix has larger energy range (from 5 keV), it showed a lower
760 absorbed dose than the MDUs. This is difficult to explain since the Minipix was
761 calibrated against the TEPC and showed a very good agreement to the TEPC Hawk
762 low-LET part (Ploc 2009). However, it should be mentioned that the setting of
763 Timepix, especially bias, could have been different for different experiments, which
764 might have caused some discrepancies. In this flight, the bias was set to 30 V. It is
765 important to use the same conditions (parameters) for all instruments.

766 Taking the MDU7 (MDU 7 has been calibrated at CERF) energy deposition spectra
767 and performing the calibration according to (Ploc 2009), the total $H^*(10)$ rate
768 arrived at 7.1 $\mu Sv \cdot h^{-1}$, which agreed well with the TEPC results.

769 5. Conclusions

770 For the instruments with the potential to be used onboard aircraft, appropriate
771 calibration and determination of calibration/correction factor is crucial. A good
772 measurement of the atmospheric ambient dose equivalent requires that the
773 instrument response for all particles and energies is properly taken into account. As
774 there is no traceable reference field for the total radiation field in the atmosphere,
775 comparison of instruments onboard aircraft is necessary.

776 Various radiation detector systems were compared onboard aircraft under stable
777 flight conditions during the REFLECT measurement campaign – the largest
778 comparison of this type ever performed. As expected, the dosimeters routinely used
779 for aircraft dosimetry (TEPC, Liulin) worked adequately, the results agreed with
780 each other as well as with the EPCARD computer model calculations.

781 Since high-energy neutrons contribute significantly to $H^*(10)$, conventional neutron
782 rem counters (with energy range limited to about 20 MeV) underestimated neutron
783 $H^*(10)$ with standard calibration procedures using neutron sources such as AmBe
784 or Cf-252. Extended-range neutron rem counters (NM2B-495Pb, LINUS) provided
785 results comparable to $H^*(10)_n$ determined with routinely used instruments and the
786 EPCARD calculation.

The reading of some instruments (LB6419, FHZ-612B) was higher than expected from the assumption that the detector is only sensitive to a specific component of the radiation field. However, it should be noted that these instruments are not primarily intended for use onboard aircraft in a very complex mixed radiation field. Their response to the various components of the cosmic radiation field and the energy dependence still need to be fully characterised.

The REFLECT campaign enabled measurement in uniform, well-defined conditions onboard an aircraft and comparison of new instruments with those routinely used. Although the response of some instruments, not primarily intended for the use in a very complex mixed radiation field such as onboard aircraft, was different than as somehow expected, more experiments are necessary too finally declare them as not suitable. This campaign consisted only of one flight with one set of parameters (vertical cut-off rigidity, altitude, phase of solar cycle) and it was relatively short. For further testing of instruments showing some potential to be used for routine dosimetry onboard aircraft, additional flights at different geomagnetic cut-offs and altitudes as well as comparison at appropriate reference fields (CERF) are needed. The REFLECT provided valuable experience enabling to discuss some issues connected with the use of the dosimeters in such complex radiation field and it also provided feedback for designing future in-flight campaigns.

Acknowledgements

The research flight has been part of the research activities of the CRREAT (Research Center of Cosmic Rays and Radiation Events in the Atmosphere) project funded by the European Structural and Investment Funds under the Operational Program Research, Development and Education (CZ.02.1.01/0.0/0.0/15_003/0000481).

This work was carried out within the European Radiation Dosimetry Group (EURADOS, WG11 High energy radiation fields).

We would like to thank ABSJets pilots and technicians for their assistance during the flight and its preparation.

References

Andersson, I.O., Braun, J.A. 1963. Neutron rem-counter with uniform sensitivity from 0.025 eV to 10 MeV. *Proceedings of the IAEA Symposium on Neutron dosimetry*. IAEA. Vienna. Vol. **II**: 87-95.

Badhwar, G. D. 1997. The radiation environment in low-Earth orbit. *Radiat. Res.* **148**: 3–10. doi:10.2307/3579710

Badhwar, G.D., O'Neill, P.M., Troung, A.G. 2000. Galactic cosmic radiation environmental models, private communication.

Battistoni, G., Ferrari, A., Pelliccioni, M. and Villari, R. 2005. Evaluation of the doses to aircrew members taking into consideration the aircraft structures. *Adv. Space Res.* **36**: 1645–1652 . doi:10.1016/j.asr.2005.04.037

Beck, P. 2009. Overview of research on aircraft crew dosimetry during the last solar cycle. *Radiation Protection Dosimetry* **136**: 244-250. doi:10.1093/rpd/ncp158

Beck, P., Latocha, M., Rollet, S., Stehno G. 2005. TEPC reference measurements at aircraft altitudes during a solar storm. *Adv. Space Res.* **36**: 1627-1633. doi:10.1016/j.asr.2005.05.035

Bengtsson, L. G. 1970. Assessment of Dose Equivalent from Fluctuation of Energy Depositions. *Proc. 2nd Symp. on Microdosimetry EUR-4552 (Brussels: CEC)*: 375–400.

Bergmeier, F., Volnhals, M., Wielunski, M., Rühm, W. 2013. Simulation and calibration of an active neutron dosemeter. *Radiat. Prot. Dosim.* **161**: 126–129. doi:10.1093/rpd/nct316

BERTHOLD n.d., *LB 6411 Neutron Probe*, Berthold Technologies USA, accessed 14 April 2020, <http://www.berthold-us.com/50-rad-pro-products/probes-sensors/156-lb6411.html>

Birattari, C., Ferrari, A., Nuccetelli, C., Pelliccioni, M., Silari, M. 1990. An extended range neutron rem counter. *Nuclear Instruments and Methods in Physics Research* **A 297**: 250-257. doi: 10.1016/0168-9002(90)91373-J

Birattari, C., Esposito, A., Ferrari, A., Pelliccioni, M., Silari, M. 1992. A neutron survey-meter with sensitivity extended up to 400 MeV. *Radiation Protection Dosimetry* **44**: 193-197. doi: 10.1093/rpd/44.1-4.193

845 Birattari, C., Esposito, A., Ferrari, A., Pelliccioni, M., Silari, M. 1993. Calibration of the
846 neutron rem counter LINUS in the energy range from thermal to 19 MeV. *Nuclear*
847 *Instruments and Methods in Physics Research* **A 324**: 232-238. doi: 10.1016/0168-
848 9002(93)90982-N

849 Birattari, C., Esposito, A., Ferrari, A., Pelliccioni, M., Rancati, T., Silari, M. 1998. The
850 extended range Neutron rem counter 'LINUS': overview and latest developments.
851 *Radiation Protection Dosimetry* **76**: 135-148. doi:
852 10.1093/oxfordjournals.rpd.a032258

853 Böhlen, T.T., Cerutti, F., Chin, M.P.W., Fassò, A., Ferrari, A., Ortega, P.G., Mairani, A.,
854 Sala, P.R., Smirnov, G., Vlachoudis, V. 2014. The FLUKA Code: Developments and
855 Challenges for High Energy and Medical Applications. *Nuclear Data Sheets* **120**: 211-
856 214. doi: 10.1016/j.nds.2014.07.049

857 Bottollier-Depois, J.-F., Trompier, F., Clairand, I., Spurny, F., Bartlett, D., Beck, P.,
858 Lewis, B., Lindborg, L., O'Sullivan, D., Roos, H., Tommasino, L. 2004. Exposure of
859 aircraft crew to cosmic radiation: on-board intercomparison of various dosemeters,
860 *Radiation Protection Dosimetry* **110**: 411–415. doi: 10.1093/rpd/nch217

861 Bottollier-Depois, J.F., Beck, P., Latocha, M., Mares, V., Matthiä, D., Rühm, W.,
862 Wissmann, F. 2012. Comparison of Codes Assessing Radiation Exposure of Aircraft
863 Crew due to Galactic Cosmic Radiation. *EURADOS Report* **2012-03**, Braunschweig,
864 May 2012. ISBN 978-3-943701-02-9

865 Bottollier-Depois, J.F., Allain, E., Baumont, G., Berthelot, N., Darley, G., Ecrabet, F.,
866 Jolivet, T., Lebeau-Livé, A., Lejeune, V., Quéinnec, F., Simon, C., Trompier, F. 2019. The

867 OpenRadiation project: monitoring radioactivity in the environment by and for the
868 citizens. *Radioprotection* **54**, 241-246. doi: 10.1051/radiopro/2019046

869 Burgkhardt, B., Fieg, G., Klett, A., Plewnia, A., Siebert B.R.L. 1997. The neutron
870 fluence and H*(10) response of the new LB 6411 rem counter. *Radiat. Prot. Dos.* **70**:
871 361-364. doi: 10.1093/oxfordjournals.rpd.a031977

872 Campbell, M. On behalf of all members of the Medipix2 Collaboration. 2011. 10 years
873 of the Medipix2 Collaboration. *Nuclear Instruments and Methods in Physics Research*
874 *Section A: Accelerators, Spectrometers, Detectors and Associated Equipment* **633**: S1-
875 S10. doi: 10.1016/j.nima.2010.06.106

876 Caresana, M., Denker, A., Esposito, A., Ferrarini, M., Golnik, N., Hohmann, E.,
877 Leuschner, A., Luszik-Bhadra, M., Manessi, G., Mayer, S., Ott, K., Röhrich, J., Silari, M.,
878 Trompier, F., Volnhals, M., Wielunski, M. 2014. Intercomparison of radiation
879 protection instrumentation in a pulsed neutron field. *Nuclear Instruments and*
880 *Methods in Physics Research Section A: Accelerators, Spectrometers, Detectors and*
881 *Associated Equipment* **737**: 203-213. doi: 10.1016/j.nima.2013.11.073

882 Conroy, T. 2004. FWT Far West Technology Inc., Environmental radiation monitor
883 with 500 Tissue Equivalent Proportional Counter (TEPC), HAWK Version 2.
884 *Operations and Repair Manual*, Far West Technology, Inc., Goleta, USA.

885 CRREAT n.d., *The CRREAT project,* Nuclear Physics Institute CAS, accessed 14 April,
886 2020, < http://www.ujf.cas.cz/en/research-development/large-research-
887 infrastructures-and-centres/crreat/objectives/>

888 Dachev, T.P. 2009. Characterization of the near Earth radiation environment by
889 Liulin type spectrometers. *Adv. Space Res.* **44**: 1441–1449. doi:
890 10.1016/j.asr.2009.08.007

891 Dinar, N., Pozzi, F., Silari, M. 2017. Characterization of the LINUS detector. *CERN*
892 *Technical Note*, EDMS 1822865.

893 Dwyer, J. R., Smith, D. M., Uman, M. A., Saleh, Z., Grefenstette, B., Hazelton, B., Rassoul,
894 H. K. 2010. Estimation of the fluence of high-energy electron bursts produced by
895 thunderclouds and the resulting radiation doses received in aircraft. *Journal of*
896 *Geophysical Research* **115**, D09206. doi: 10.1029/2009JD012039

897 EPCARD 2020, *EPCARD online,* Helmholtz Zentrum Muenchen, accessed 14 April
898 2020, <https://www.helmholtz-muenchen.de/epcard>

899 EURADOS 1996. Exposure of Air Crew to Cosmic Radiation. I.R. McAulay, D.T.
900 Bartlett, G. Dietre, H.G. Menzel, K. Schnuer, H.J. Schrewe (Eds.), Luxembourg, ISBN
901 92-827-7994-7.

902 EURADOS 2020, *The European Radiation Dosimetry Group,* EURADOS, accessed 14
903 April 2020, < https://eurados.sckcen.be/en>

904 EURATOM 1996. Council Directive 96/29/EURATOM of 13 May 1996 laying down
905 the basic safety standards for protection of the health of workers and the general
906 public against the dangers arising from ionising radiation. *Official J. European*
907 *Communities*, 39, L159.

908 EURATOM 2013. Council Directive 2013/59/EURATOM of 5 December 2013 laying
909 down basic safety standards for protection against the dangers arising from exposure to

ionising radiation, and repealing Directives 89/618/Euratom, 90/641/Euratom, 96/29/Euratom, 97/43/Euratom and 2003/122/Euratom. *OJ L 13, 17.1.2014.*

Farah, J., De Saint-Hubert, M., Mojżeszek, N., Chiriotti, S., Gryzinski, M., Ploc, O., Trompier, F., Turek, K., Vanhavere, F., Olko, P. 2017. Performance tests and comparison of microdosimetric measurements with four tissue-equivalent proportional counters in scanning proton therapy. *Radiat. Meas.* **96**: 42-52. doi: 10.1016/j.radmeas.2016.12.005

Federico, C.A., Goncalez, O.L., Caldas, L.V.E., Pazianotto, M.T., Dyer, C., Caresana, M., Hands, A. 2015. Radiation measurements onboard aircraft in the South Atlantic region. *Radiat. Meas.* **82**: 14-20. doi: 10.1016/j.radmeas.2015.07.008

Ferrari, A., Pelliccioni, M., Villari, R. 2004. Evaluation of the influence of aircraft shielding on the aircrew exposure through an aircraft mathematical model. *Radiat. Prot. Dosimetry* **108**: 91–105. doi: 10.1093/rpd/nch008

Ferrari, A., Sala, P.R., Fasso, A., Ranft, J. 2005. FLUKA: A Multi Particle Transport Code. CERN-2005-010, SLAC-R-773, INFN-TC-05-11. doi: 10.2172/877507

GitHub 2020, *ODZ-UJF-AV-CR/AIRDOS01: Airborne cosmic radiation dosimeter*, GitHub, Inc., accesses 14 April 2020, <https://github.com/ODZ-UJF-AV-CR/AIRDOS>

Golnik, N. 2018. Recombination chambers - do the old ideas remain useful? *Radiation Protection Dosimetry* **180**: 3–9. doi: 10.1093/rpd/ncx279

Golnik, N., Mayer, S., Zielczyński, M. 2004. Recombination index of radiation quality of low-LET radiation. *Nuclear Instruments and Methods in Physics Research Section B:*

Beam Interactions with Materials and Atoms **213**: 650-653. doi: 10.1016/S0168-583X(03)01679-3

Granja, C., Pospisil, S. 2014. Quantum dosimetry and online visualization of X-ray and charged particle radiation in commercial aircraft at operational flight altitudes with the pixel detector Timepix. *Advances in Space Research* **54**: 241–251. doi: 10.1016/j.asr.2014.04.006

Granja, C., Kudela, K., Jakubek, J., Krist, P., Chvatil, D., Stursa, J., Polansky, S. 2018. Directional detection of chargedparticles and cosmic rays with the miniaturized radiation camera MiniPIX timepix. *Nuclear Instruments and Methods in Physics Research Section A: Accelerators, Spectrometers, Detectors and Associated Equipment* **911**: 142-152. doi: 10.1016/j.nima.2018.09.140

IAEA 1995. Atomic and molecular data for radiotherapy and radiation research. IAEA-TECDOC-799.

IAEA 2001. Compendium of neutron spectra and detector responses for radiation protection purposes: Supplement to technical report series, No.318, IAEA Technical Reports Series No. 403.

IAEA 2003. Occupational Radiation Protection: Protecting Workers Against Exposure to Ionizing Radiation. Proceedings of an International Conference Held in Geneva, Switzerland, 26–30 August 2002. STI/PUB/1145.

ICRP, 1991. 1990 Recommendations of the International Commission on Radiological Protection. ICRP Publication 60. Ann. ICRP 21 (1-3).

ICRP, 1997. General Principles for the Radiation Protection of Workers. ICRP Publication 75. Ann. ICRP 27 (1).

ICRP 2007. The 2007 Recommendations of the international commission on radiological protection. ICRP publication 103.

ICRP 2016. Radiological Protection from Cosmic Radiation in Aviation. ICRP Publication 132. Ann. ICRP 45(1), 1–48.

ICRU 1983. International Commission on Radiation Units and Measurements; Bethesda, MD: 1983. Microdosimetry. Report 36.

ICRU 1993. Quantities and Units in Radiation Protection Dosimetry. ICRU Report 51, ICRU Publications: Bethesda

ICRU 2010. Reference Data for the Validation of Doses from Cosmic-Radiation Exposure of Aircraft Crew. ICRU Report 84 (prepared jointly with ICRP). Journal of the ICRU 10 (2).

ISO 1999. X and gamma reference radiation for calibrating dosemeters and doserate meters and for determining their response as a function of photon energy — Part 3: Calibration of area and personal dosemeters and the measurement of their response as a function of energy and angle of incidence. ISO 4037-3:1999.

ISO 2001. Reference neutron radiations — Part 1: Characteristics and methods of production. ISO 8529-1:2001.

ISO 2012. Dosimetry for exposures to cosmic radiation in civilian aircraft — Part 1: Conceptual basis for measurements. ISO 20785-1:2012.

974 Jakubek, J. 2011. Precise energy calibration of pixel detector working intime-over-
975 threshold mode. *Nuclear Instruments and Methods in Physics Research A* **633**: S262-
976 S266. doi:10.1016/j.nima.2010.06.183

977 Kákona, M., Štěpán, V., Ambrožová, I., Arsov, T., Chroust, J., Kákona, J., Kalapov, I.,
978 Krist, P., Lužová, M., Nikolova, N., Peksová, D., Ploc, O., Sommer, M., Šlegl, J., Angelov,
979 C. 2019. Comparative Measurements of Mixed Radiation Fields Using Liulin and
980 AIRDOS Dosimeters. AIP Conference Proceedings 2075, 130003. doi:
981 10.1063/1.5091288

982 Kellerer, A.M. 1968 Mikrodosimetrie GSF-Bericht B-1 (Forschungszentrum für
983 Umwelt und Gesundheit).

984 Kellerer, A. M, Rossi, H.H. 1984. On the Determination of Microdosimetric
985 Parameters in Time-Varying Radiation Fields: the Variance-Covariance Method.
986 *Radiat. Res.* **97**: 237–245. doi: 10.2307/3576275

987 Kyllönen, J-E., Lindborg, L., Samuelson, G. 2001a. The response of the Sievert
988 instrument in neutron beams up to 180 MeV. *Radiat. Prot. Dosim.* **94**(3): 227-232.
989 doi: 10.1093/oxfordjournals.rpd.a006494

990 Kyllönen, J-E., Lindborg, L., Samuelson, G. 2001b Cosmic Radiation Measurements
991 on-board aircraft with the variance method. *Radiation Prot. Dosim.* **93**(3): 197-205.
992 doi: 10.1093/oxfordjournals.rpd.a006430

993 Kubančák, J., Ambrožová, I., Ploc, O., Brabcová, K. P., Štěpán, V., Uchihori, Y. 2014.
994 Measurement of dose equivalent distribution on board commercial jet aircraft.
995 *Radiat. Prot. Dos.* **162**: 215-219. doi:10.1093/rpd/nct331

996 Kubančák, J., Ambrožová, I., Pachnerová Brabcová, K., Jakůbek, J., Kyselová, D., Ploc,
997 O., Bemš, J., Štěpán, V., Uchihori, Y. 2015. Comparison of cosmic rays radiation
998 detectors on-board commercial jet aircraft. *Radiat. Prot. Dosimetry* **164**: 484-488.
999 doi:10.1093/rpd/ncv331

1000 Latocha, M., Autischer, M., Beck, P., Bottolier-Depois, J.F., Rollet, S., Trompier, F.
1001 2007. The results of cosmic radiation in-flight TEPC measurements during the
1002 CAATER flight campaign and comparison with simulation. *Radiat. Prot. Dosim*. **125**
1003 (1-4): 412-415. doi: 10.1093/rpd/ncl123

1004 Leake, J.W. 1966. A spherical dose equivalent neutron detector. *Nuclear Instruments*
1005 *and Methods* **45**: 151-156. doi: 10.1016/0029-554X(66)90420-4

1006 Leake, J.W. 2004. Improvements to the Leake Neutron Detector I. *Nuclear*
1007 *Instruments and Methods in Physics Research Section A: Accelerators, Spectrometers,*
1008 *Detectors and Associated Equipment* **519**(3): 636-646. doi:
1009 10.1016/j.nima.2003.11.040

1010 Leuschner, A., Asano, Y., Klett, A. 2017. Calibration of the radiation monitors from
1011 DESY and SPring-8 at the quasi-mono-energetic neutron beams using 100 and 300
1012 MeV ^{7}Li(p,n) reaction at RCNP in Osaka Japan in November 2014. *EPJ Web of*
1013 *Conferences* **153**: 08017. doi: 10.1051/epjconf/201715308017

1014 Lillhök , J.E. 2007. The microdosimetric variance-covariance method used for beam
1015 quality characterization in radiation protection and radiation therapy. PhD thesis.
1016 ISBN 91-7155-391-6

1017 Lillhök, J., Beck, P., Bottollier-Depois, J.F., Latocha, M., Lindborg, L., Roos, H., Roth, J.,
1018 Schraube, H., Spurny, F., Stehno, G., Trompier, F., Wissmann, F. 2007. A comparison
1019 of ambient dose equivalent meters and dose calculations at constant flight
1020 conditions. *Radiat. Meas.* **42**: 323–333. doi: 10.1016/j.radmeas.2006.12.011

1021 Lillhök, J., Persson, L., Andersen, C.E., Dasu, A., Ardenfors, O. 2017 Radiation
1022 protection measurements with the variance-covariance method in the stray
1023 radiation fields from photon and proton therapy facilities. *Radiat. Prot. Dosimetry*
1024 **180**(1-4): 338-341. doi: 10.1093/rpd/ncx194

1025 Lindborg, L., Bengtsson, L.G. 1971. Development of a microdosimetry system for use
1026 with high energy electron beams. *Proceedings of the Third Symposium on*
1027 *Microdosimetry*, EUR 4810 d-f-e.

1028 Lindborg, L., Kyllönen, J.E., Beck, P., Bottolier, J.F., Gerdung, S. 1999. The use of TEPC
1029 for Reference Dosimetry. *Radiat. Prot. Dosim.* **86**: 285-288. doi:
1030 10.1093/oxfordjournals.rpd.a032959

1031 Lindborg, L., Bartlett, D.T., Beck, P., McAulay, I.R., Schnuer, K., Schraube, H., Spurny,
1032 F. 2004. Cosmic radiation exposure of aircraft crew: compilation of measured and
1033 calculated data. Final report of the EURADOS WG 5. European Commission,
1034 Directorate-General for Energy and Transport, Radiation Protection Issue No. 140,
1035 Luxembourg, ISBN 92-894-8448-9

1036 Lindborg, L., Beck, P., Bottolier-Depois, J.F., Latocha, M., Lillhök, J., Rollet, S., Roos, H.,
1037 Roth, J., Schraube, H., Spurny, F., Stehno, G., Trompier, F., Wissmann, F. 2007.

1038 Determinations of H*(10) and its dose components onboard aircraft. *Radiat. Prot.*
1039 *Dosim*. **126** (1-4): 577-580. doi: 10.1093/rpd/ncm117

1040 Llopart, X., Campbell, M., Dinapoli, R., San Segundo, D., Pernigotti, E. 2002. Medipix2:
1041 a 64-k Pixel readout Chip with 55-um Square Elements Working in Single Photon
1042 Counting Mode. *IEEE transactions on nuclear science* **49(5)**: 2279-2283.
1043 doi:10.1109/TNS.2002.803788

1044 Llopart, X., Ballabriga, R., Campbell, M., Tlustos, L., Wong, W. 2007. Timepix, a 65k
1045 programmable pixel readout chip for arrival time, energy and/or photon counting
1046 measurements. *Nuclear Instruments and Methods in Physics Research Section A:*
1047 *Accelerators, Spectrometers, Detectors and Associated Equipment* **581**: 485-494. doi:
1048 10.1016/j.nima.2007.08.079

1049 Maciak, M. 2018. Calculation of LET distributions in the active volume of a
1050 recombination chamber. *Radiation Protection Dosimetry* **180**(1-4): 407–412. doi:
1051 10.1093/rpd/ncy073

1052 Mares, V., Sannikov, A.V., Schraube, H. 2002. Response function of the Anderson-
1053 Braun and extended range rem counters for neutron energies from thermal to 10
1054 GeV. *Nucl. Instrum. Methods Phys. Res., Sect. A* **476**: 341–346. doi: 10.1016/S0168-
1055 9002(01)01459-0

1056 Mares, V., Roesler, S., Schraube, H. 2004. Averaged particle dose conversion
1057 coefficient in air crew dosimetry. *Radiat. Prot. Dosim.* **110**(1-4): 371-376. doi:
1058 10.1093/rpd/nch137

1059 Mares, V., Leuthold, G. 2007. Altitude-dependent dose conversion coefficients in
1060 EPCARD. *Radiation Protection Dosimetry* **126**(1-4): 581-584. doi:
1061 10.1093/rpd/ncm118

1062 Mares, V., Maczka, T., Leuthold, G. Rühm, W. 2009. Air crew dosimetry with a new
1063 version of EPCARD. *Radiat. Prot. Dosim.* **136**(4): 262-266. doi: 10.1093/rpd/ncp129

1064 Mares, V., Trinkl, S., Iwamoto, Y., Masuda, A., Matsumoto, T., Hagiwara, M., Satoh, D.,
1065 Yashima, H., Shima, T., Nakamura, T. 2017. Neutron spectrometry and dosimetry in
1066 100 and 300 MeV quasimono-energetic neutron field at RCNP, Osaka University,
1067 Japan. *EPJ Web of Conferences* **153**, 08020. doi: 10.1051/epjconf/201715308020

1068 Meier, M.M., Hubiak, M., Matthiä, D., Wirtz, M., Reitz, G. 2009. Dosimetry at aviation
1069 altitudes (2006–2008). *Radiat. Prot. Dosim.* **136** (4): 251–255. doi:
1070 10.1093/rpd/ncp142

1071 Meier, M.M, Trompier, F., Ambrozova, I., Kubancak, J., Matthia, D., Ploc, O., Santen, N.,
1072 Wirtz, M. 2016. CONCORD: comparison of cosmic radiation detectors in the
1073 radiation field at aviation altitudes. *J. Space Weather Space Clim.* **6**, A24. doi:
1074 10.1051/swsc/2016017

1075 Meier, M.M., Copeland, K., Matthia, D., Mertens, C.J., Schennetten, K. 2018. First Steps
1076 Toward the Verification of Models for the Assessment of the Radiation Exposure at
1077 Aviation Altitudes During Quiet Space Weather Conditions. *Space Weather* **16**: 1269-
1078 1276. doi: 10.1029/2018SW001984

1079 Murawski, Ł., Maciak, M., Gryziński, M.A., Domański, S. 2018. Investigation on
1080 radiation shielding properties of special concrete in neutron fields. *Radiation*
1081 *Protection Dosimetry* **180**(1-4): 413–416, https://doi.org/10.1093/rpd/ncy012

1082 Pazianotto, M.T., Cortes-Giraldo, M.A., Federico, C.A., Hubert, G., Goncalez, O.L.,
1083 Quesada, J.M., Carlson, B.V. 2017. Extensive air shower Monte Carlo modeling at the
1084 ground and aircraft flight altitude in the South Atlantic Magnetic Anomaly and
1085 comparison with neutron measurements. *Astroparticle Physics* **88**: 17-29. doi:
1086 10.1016/j.astropartphys.2016.12.004

1087 Operational Procedure M-1: Measurement of dose equivalent in mixed radiation
1088 field with REM-2 recombination chamber, Radiation Protection Measurements
1089 Laboratory, National Centre for Nuclear Research, 15 March 2017.

1090 Ploc, O. 2009. Measurement of Exposure to Cosmic Radiation at Near-Earth Vicinity
1091 with Energy Deposition Spectrometer Liulin onboard Aircrafts and Spacecrafts. PhD
1092 thesis, Czech Technical University in Prague.

1093 Ploc, O., Brabcova, K., Spurny, F., Malusek, A., Dachev, T. 2011. Use of energy
1094 deposition spectrometer Liulin for individual monitoring of aircrew. *Radiat. Prot.*
1095 *Dosim.* **144**: 611–614. doi: 10.1093/rpd/ncq505

1096 Ploc, O., Ambrozova, I., Kubancak, J., Kovar, I., Dachev, T.P. 2013. Publicly available
1097 database of measurements with the silicon spectrometer Liulin onboard aircraft.
1098 *Radiat. Meas.* **58**: 107–112. doi: 10.1016/j.radmeas.2013.09.002

1099 Pozzi, F., Carbonez, P., Macián-Juan, R. 2015. CERN Radiation Protection (RP)
1100 calibration facilities. CERN-THESIS-2015-394.

Pozzi, F., Garcia Alia, R., Brugger, M., Carbonez, P., Danzeca, S., Gkotse, B., Jaekel, M.R., Ravotti, F., Silari, M., Tali, M. 2017. CERN irradiation facilities. *Radiation Protection Dosimetry* **80**(1-4): 120-124. doi: 10.1093/rpd/ncx187

Pozzi, F. and Silari, M. 2019. The CERN-EU high-energy Reference Field (CERF) facility: new FLUKA reference values of spectral fluences, present and newly proposed operational quantities, submitted for publication in NIM A.

Pszona, S., Bantsar, A., Tulik, P., Wincel, K., Zaręba, B. 2014. Low-level gamma and neutron monitoring based on use of proportional counter filled with 3He in polythene moderator: study of the responses to gamma and neutrons. *Radiation Protection Dosimetry* **161**(1-4): 237–240. doi: 10.1093/rpd/nct274

Roesler, S., Heinrich, W., Schraube, H. 1998. Calculation of Radiation Fields in the Atmosphere and Comparison to Experimental Data. *Radiat. Res.* **149**(1): 87-97. doi: 10.2307/3579685

Roesler, S., Heinrich, W., Schraube, H. 2002. Monte Carlo calculation of the radiation field at aircraft altitudes. *Radiat. Prot. Dosim.* **98**(4): 367-388. doi: 10.1093/oxfordjournals.rpd.a006728

Silari, M., Pozzi, F. 2017. The CERN-EU high-energy Reference Field (CERF) facility: applications and latest developments. *EPJ Web of Conferences* **153**, 03001. doi: 10.1051/epjconf/20171530

Schraube H., Heinrich W., Leuthold G., Mares V., Roesler S. (2000), Aviation route dose calculation and its numerical basis (2000). In: Proc. 10th International

1122 Congress of the International Radiation Protection Association IRPA, Hiroshima,
1123 Japan (May 2000). Paper T-4-4, pp.1-9.

1124 Schraube, H., Heinrich, W., Leuthold, G., Roesler, S., and Schraube, G. 2002a. Collating
1125 of data for the determination of the exposure of aviation personnel due to cosmic
1126 radiation, concluded by 21 Dec 2000, and Calculation of radiation fields at air craft
1127 flight altitude during the period of solar maximum activity by 15 Nov 2000. Joint
1128 Report to The Council of the Dublin Institute for Advanced Studies (DIAS) 2002.

1129 Schraube, H., Leuthold, G., Heinrich, W., Roesler, S., Mares, V., Schraube, G. 2002b.
1130 EPCARD – European program package for the calculation of aviation route doses,
1131 User's manual. GSF-National Research Center, Neuherberg, Germany (2002). ISSN
1132 0721 - 1694. GSF-Report 08/02

1133 Tagziria, H., Tanner, R.J., Bartlett, D.T., Thomas, D.J. 2004. Evaluation and Monte
1134 Carlo modelling of the response function of the Leake neutron area survey
1135 instrument. *Nuclear Instruments and Methods in Physics Research Section A:*
1136 *Accelerators, Spectrometers, Detectors and Associated Equipment* **531**(3): 596-606.
1137 doi: 10.1016/j.nima.2004.05.086

1138 Tobiska, W.K., Atwell, W., Beck, P., Benton, E., Copeland, K., Dyer, C., Gersey, B.,
1139 Getley, I., Hands, A., Holland, M., Hong, S., Hwang, J., Jones, B., Malone, K., Meier, M.M.,
1140 Mertens, C., Phillips, T., Ryden, K., Schwadron, N., Wender, S.A., Wilkins, R., Xapsos,
1141 M.A. 2015. Advances in atmospheric radiation measurements and modeling needed
1142 to improve air safety. *Space Weather* **13**: 202–210. doi: 10.1002/2015SW001169

1143 Trompier, F., Delacroix, S., Vabre, I., Joussard, F., Proust, J. 2007. Secondary exposure
1144 for 73 and 200 MeV proton therapy. *Radiat. Prot. Dosim.* **125**(1-4): 349-354. doi:
1145 10.1093/rpd/ncm154

1146 Turecek, D., Jakubek, J. 2015. PIXET Software package tool for control, readout and
1147 online display ofpixel detectors Medipix/Timepix, Advacam, Prague.

1148 Volnhals, M., 2012. Improvement of the HMGU Neutron Dosemeter by Monte Carlo
1149 Simulations and Measurements. Diploma Thesis, TU Munich.

1150 Wielunski, M., Schutz, R., Fantuzzi, E., Pagnamenta, A., Wahl, W., Palfalvi, J., Zombori,
1151 P., Andrasi, A., Stadtmann, H., Schmitzer, C. 2004. Study of the sensitivity of neutron
1152 sensors consisting of a converter plus Si charged-particle detector. *Nucl. Instr. And*
1153 *Meth. A* **517**: 240–253. doi: 10.1016/j.nima.2003.07.032

1154 Wielunski, M., Brall, T., Dommert, M., Trinkl, S., Rühm, W., Mares, V. 2018. Electronic
1155 neutron dosimeter in high-energy neutron fields. *Radiation Measurements* **114**: 12-
1156 18. doi: 10.1016/j.radmeas.2018.04.015

1157 Wissmann, F., Klages, T. 2018. A simple method to monitor the dose rate of
1158 secondary cosmic radiation at altitude. *J. Radiol. Prot.* **39**: 71-84. doi: 10.1088/1361-
1159 6498/aaeeae

1160 Yasuda, H., Yajima, K. 2018. Verification of cosmic neutron doses in long-haul flights
1161 from Japan. *Radiat. Meas.* **119**: 6-11. doi: 10.1016/j.radmeas.2018.08.016

1162 Yasuda, H., Yajima, K., Sato, T. 2020. Investigation of using a long-life electronic
1163 personal dosimeter for monitoring aviation doses of frequent flyers. *Radiat. Meas*.

Available online 20 March 2020, 106309, in press. doi: 10.1016/j.radmeas.2020.106309

Uchihori, Y., Kitamura, H., Fujitaka, K., Dachev, T.P., Tomov, B.T., Dimitrov, P.G., Matviichuk, Y. 2002. Analysis of the calibration results obtained with Liulin-4J spectrometer–dosimeter on protons and heavy ions. *Radiat. Meas.* **35**: 127-134. doi: 10.1016/S1350-4487(01)00286-4

Zielczynski, M., Golnik, N. 1994. Recombination Index of Radiation Quality - Measuring and Applications. *Radiation Protection Dosimetry* **52**(1-4): 419–422. doi: 10.1093/oxfordjournals.rpd.a082226

Zielczyński M., Golnik N., Gryziński M.A. 2008. Applications of recombination chambers in the dosimetry of high energy radiation fields. *NUKLEONIKA* **53**(suppl. 1): S45–S52.